OPEN ACCESS

J. Integr. Neurosci.

Case study

QEEG-based neural correlates of decision making in a well-trained eight year-old chess player

Abolfazl Alipour[1,2], Sahar Seifzadeh[3], Hadi Aligholi[2,4], Mohammad Nami[2,4,5,*]

[1] Department of Psychological and Brain Sciences, Indiana University, Bloomington, Indiana, USA
[2] Neuroscience Laboratory-NSL (Brain, Cognition and Behavior), Department of Neuroscience, School of Advanced Medical Sciences and Technologies, Shiraz University of Medical Sciences, Shiraz, Iran
[3] Young Researchers and Elite Club, Qazvin Branch, Islamic Azad University, Qazvin, Iran
[4] Department of Neuroscience, School of Advanced Medical Sciences and Technologies, Shiraz University of Medical Sciences, Shiraz, Iran
[5] Clinical Neurology Research Center, Shiraz University of Medical Sciences, Shiraz, Iran

*Correspondence: torabinami@sums.ac.ir (Mohammad Nami)

https://doi.org/10.31083/JIN-170056

Abstract

The neurocognitive substrates of decision making in the context of chess has appealed to the interest of investigators for decades. Expert and beginner chess players are hypothesized to employ different functional brain networks when involved in episodes of critical decision making while playing chess. Cognitive capacities including, but not restricted to, pattern recognition, visuospatial search, reasoning, planning, and decision making are perhaps the key determinants of the reward and judgment decisions made during chess games. Meanwhile, the precise neural correlates of decision making in this context has largely remained elusive. Quantitative electroencephalography is an investigative tool possessing an appropriate temporal resolution for the study of the neural correlates of cognitive tasks at a cortical level. A 22-channel electroencephalography setup and digital polygraphy were employed in the investigation of a well-trained eight-year old boy while engaged in playing chess against a computer. Quantitative analyses mapped and source-localized electroencephalography signals. Analyses indicated a lower power spectral density for higher frequency bands in the right hemisphere during decision making related epochs. Moreover, in the given subject, the information flow of decision making blocks tended to move from posterior towards anterior brain regions.

Keywords

Chess; decision making; QEEG; electroencephalography; power spectra; functional connectivity

Submitted: September 9, 2017; **Accepted:** October 13, 2017

1. Introduction

Decision making (DM), characterized as the act of selecting the best among different alternatives, plays a defining role in various aspects of life. Complex human cognition, such as DM under uncertainty, is represented by dynamic spatio-temporal activity in the brain [1]. While so-called wise and informed decisions may contribute to success and satisfaction, ill-advised decisions often lead to failure. The multifaceted process of decision making is potentially linked to a wide range of variables including input, process, output, and feedback [2, 3].

A popular strategy board game like chess provides a compact and easily controllable task environment for the study of decision making. As such, many investigators have become attracted to chess as the task paradigm of choice for the assessment of the neural dynamics of various mental and cognitive skills including DM [4–7]. Several decades ago, a landmark study of chess players was undertaken by de Groot [4]. Key findings postulated that expertise in chess was determined more by pattern recognition than search. The general perception of the cognitive mechanisms involved in critical DM in the context of chess has been largely transformed since that study.

Subsequently, results from other investigations [8, 9] suggested that intelligence plays a key role both in DM and reasoning. On this basis, some studies have proposed a solid correlation between intelligence quotient scores and the reasoning capacity of individuals [10]. With regard to processing speed, when players are forced to play faster, their ability during the game tends to be less predictive. However, expert players are shown to perform noticeably better than novice chess players in terms of rapid object recognition abilities [11, 12].

There is a growing trend, especially among young adolescents, to join chess clubs. However, the answer as to whether playing chess may improve global DM skills, remains elusive. It is still a matter of debate as to whether, and how, playing chess may empower the adolescent brain to be more productive and error free, fast, wise, and rewarding DM.

If quantitative electroencephalography (QEEG) provides new insights about the cortical brain regions involved in critical DM among expert chess players, new avenues may be opened for DM chess related research. Potentially, through reverse engineering, cortical areas involved in a grand average QEEG of elite chess players, a path toward targeting similar networks in the brain of novice players may be defined, thus helping them to gain DM, at least in chess, in faster and more efficient ways.

The emergence of neurotechnological tools such as transcranial magnetic stimulation (TMS), transcranial direct current stimulation (tDCS) and neuro-feedback provides novel approaches for cognitive empowerment through modulation of the brain networks involved [13].

The present case study highlights results of pilot assessments concerning the neural correlates of DM at the cortical level. It employed a 22 channel-QEEG recording setup to record from a well-trained eight year-old male chess player when engaged in playing chess against a computer.

2. Case study

2.1. Subject

The subject of the case study was an eight year-old right-handed male elite chess player with both regional and national recognition in chess competitions. The subject was instructed to sleep well the night before the experiment and was not under the effect of any medicine, stimulant, food, or drink. Both the subject and legal guardian read and signed informed consent so as to participate in the study.

2.2. Experimental procedure

Subject played Chess Titans on a Windows 10 computer platform at a self-selected difficulty level (level 6) using the mouse and right hand only. Subject played the chess game for 15 minutes and was eventually defeated by the computer.

2.3. EEG recording and pre-processing

EEG was recorded while playing chess under two different conditions, including, the resting state and critical DM blocks. A 22-channel bipolar EEG montage using a 32-channel amplifier system (3840, NR-SIGN, BC, Canada) was used for QEEG data acquisition. The channel dipoles, based on the international 10-20 system, included frontopolar (FP), central (C), frontal (F), parietal (P), temporal (T), and occipital (O) electrode placements: FP2-F7, FP2-T5, F8-F3, F8-P3, F4-C3, F4-P1, T4-O1, C4-O1, T6-P1, FP1-FP2, P1-P2, FP2-C4, FP2-P2, F8-T6, F4-T4, F4-O2, T4-P4, C4-P4, T6-O2, O2-P2, O1-O2.

For the resting state condition, the subject sat in a dimly-lit recording room (320 lux) and fixated on a crosshair for ten minutes. Resting state EEG was recorded under these conditions for a duration of 10 minutes.

EEG was recorded throughout the game period. The subject verbally indicated the start of a critical DM epoch which eventually ended in moving a piece. The reported critical DM epochs ($n = 6$) were extracted for further analysis (mean duration 14 ± 4 seconds).

Simultaneous to the EEG recording, the subject was attached to a digital sampling unit for autonomic system polygraphy. This recorded real-time galvanic skin conductance (GSC) and heart rate variability (HRV) using the Vilistus DSU, UK [14] (Fig. 1).

All EEG signals were imported in EEGLAB version 13.0.0 running under MATLAB R2013a. Initial signal preprocessing included rejection of visually detectable artifacts and application of low- (1 Hz) and high-pass (48 Hz) filters. Subsequently, an Infomax-based independent component analysis (ICA) decomposition algorithm (runica.m in EEGLAB) was used to find possible artifacts. Four of 22 components were identified as artifactual (three eye movement and one muscle artifact component). After removal of these artifactual components, the ICA algorithm was used once again to obtain the final 22 artifact-free components. The obtained EEG signals were further examined with two different analysis platforms, EEGLAB and NeuroGuide (v.2.3.8, Applied Neuroscience, USA).

Fig. 1. Data acquisition setup. Subject engaged in chess against a computer. The subject reported six episodes of critical decision making during which a real-time EEG recording was marked and subsequently grand averaged in brain mapping. The galvanic skin conductance (GSC) and heart rate variability (HRV) were simultaneously monitored during the procedure with special markings indicating decision making episodes.

2.4. Topographic mapping of EEG signals

The resting state EEG, corresponding to the six critical DM epochs, was segmented into six artifact free epochs for further comparison. NeuroGuide software was used to analyze and plot topographic maps and power spectra of the EEG activity during both the resting state and critical DM epochs. The absolute and relative power of the signals in theta, alpha, and beta bands were calculated and compared between the resting state and critical DM epochs. Moreover, coherence and power ratio in the same frequency bands were computed and compared between the two states. The Wilcoxon signed-rank test was used to compare the difference between relative and absolute power spectra, power ratio, and coherence between the control and test states. Statistical significance was assumed for p values less than 0.05.

2.5. EEG source connectivity analysis

The DIPFIT2 plug-in of EEGLAB was used to source localize the EEG signals. The size of the head model was modified to match the head of the eight year-old subject based on the insights from BenAbdelkader *et al.* [15]. In short, the DIPFIT2 plug-in uses ICA components to estimate sources of EEG activity in the brain. For the 22 components existing in the signals, 22 sources were calculated. The Source Information Flow Toolbox (SIFT) [16, 17] was used to estimate the information flow between sources. In addition, the Directed Transfer Function (dDTF) [18] was used as a measure of connectivity between the 22 components. The number obtained was averaged for all time-points and all frequencies between four and 46 Hz (with two Hz intervals) in both resting state and critical DM epochs to obtain a 22×22'overall connectivity matrix'. The overall connectivity matrix of the decision making epochs was subtracted from the overall connectivity matrix of the resting state to obtain a connectivity matrix that revealed any differences in information flow between the two states. Consequently, major sink and source nodes were identified.

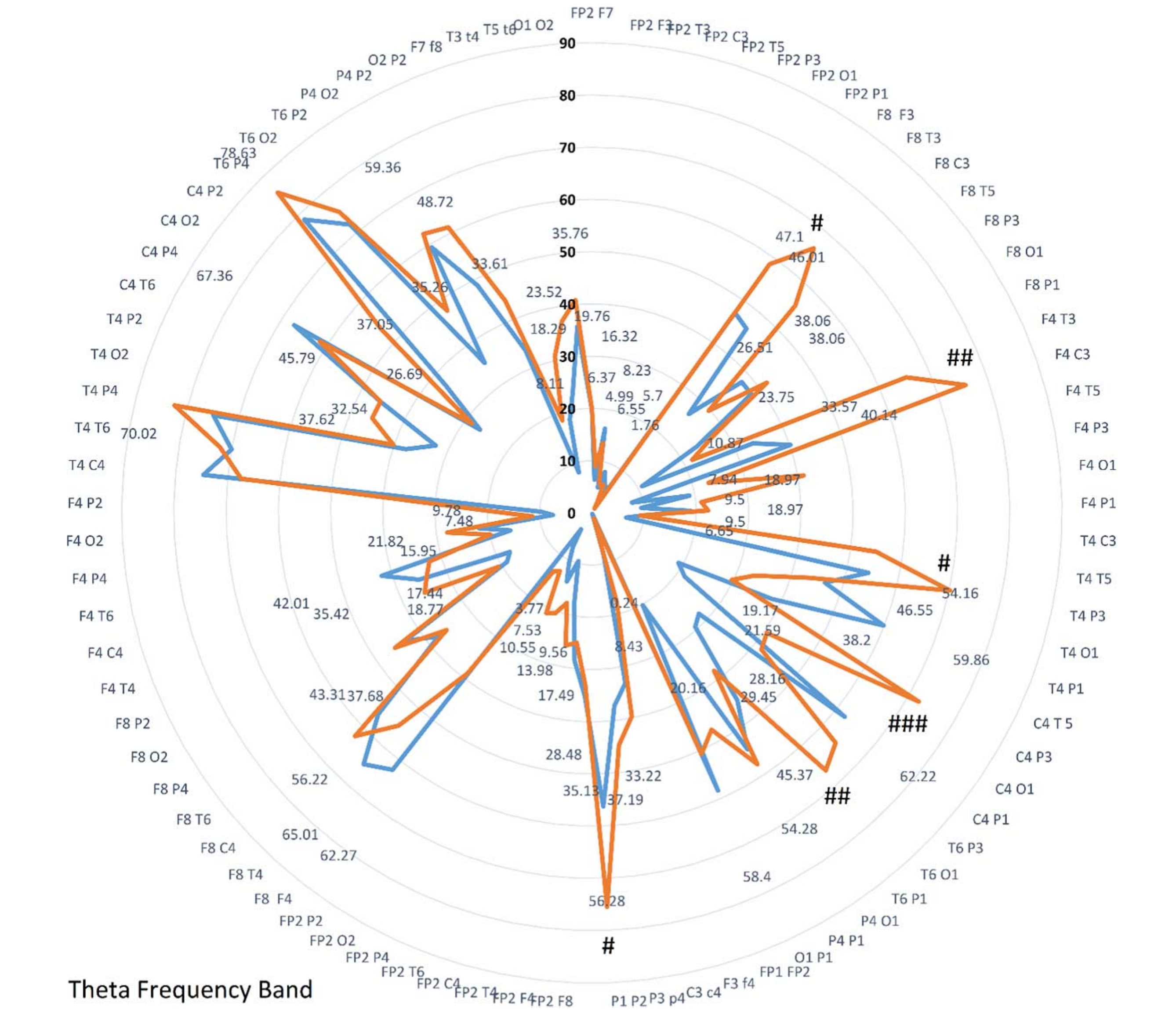

Fig. 2. Spiderweb chart plot of absolute power values for the theta frequency band upon decision making (orange) and resting state (blue) QEEG data. The analysis revealed higher theta power upon decision making task in F8-T3, F4-C3, T4-P3, C4-P3 and T6-O1 dipoles compared to resting state. Values are presented in μV^2. #$p < 0.05$, ##$p < 0.01$ and ###$p < 0.001$. FP: frontopolar, C: central, F: frontal, P: parietal, T: temporal and O: occipital.

3. Results

The grand average QEEG amplitude data for DM epochs versus resting state showed significantly higher absolute power in the range of theta and alpha frequency bands in the right frontocentral and temporoparietal brain regions upon task-positive brain cortical activity versus resting state. Furthermore, with the exception of the F4-C3 dipole, beta amplitude was less in DM states compared to the resting state.

Fig.2-Fig.4 demonstrates the comparative absolute power values for theta, alpha, and beta spectral bands. As illustrated in Fig. 2, the theta amplitude was found to significantly dominate the DM epoch grand average versus resting state QEEG for dipoles F8–T3 [$t(5) = 2.1$, 95%CI = (−1.56)–(−0.03), p = 0.03], F4–C3 [$t(5) = 2.85$, 95%CI = (−2.42)–(−0.41), p = 0.006], T4–P3 [$t(5) = 2.02$, 95%CI =(−2.26)–(−0.03), p = 0.04], C4–P3 [$t(5) = 4.48$, 95%CI (0.95)–(2.4), $p < 0.001$], and T6-O1 [$t(5) = 2.76$, 95%CI (−1.41)–(−0.005), p = 0.01].

Fig. 3 illustrates the difference in absolute power for the alpha frequency band in DM grand average epochs versus resting state for various dipole locations. Alpha amplitude was found to significantly dominate the DM epoch grand average versus resting state QEEG in F4–C3 [$t(5) = 2.93$, 95%CI = (−2.36)–(−0.71), p = 0.009]. However, F8–T3 showed a dominant alpha for the resting state compared to task-positive epochs [$t(5) = 2.22$, 95%CI = (−1.57)–(−0.08), p = 0.03].

As shown in Fig. 4, beta power was diminished in anterior brain regions for task-positive states compared with resting QEEG. In other words, unlike a higher amplitude beta for many tests of the resting state, alpha and theta amplitude assumed control of right hemisphere dipoles in the task-positive state. Based on comparative

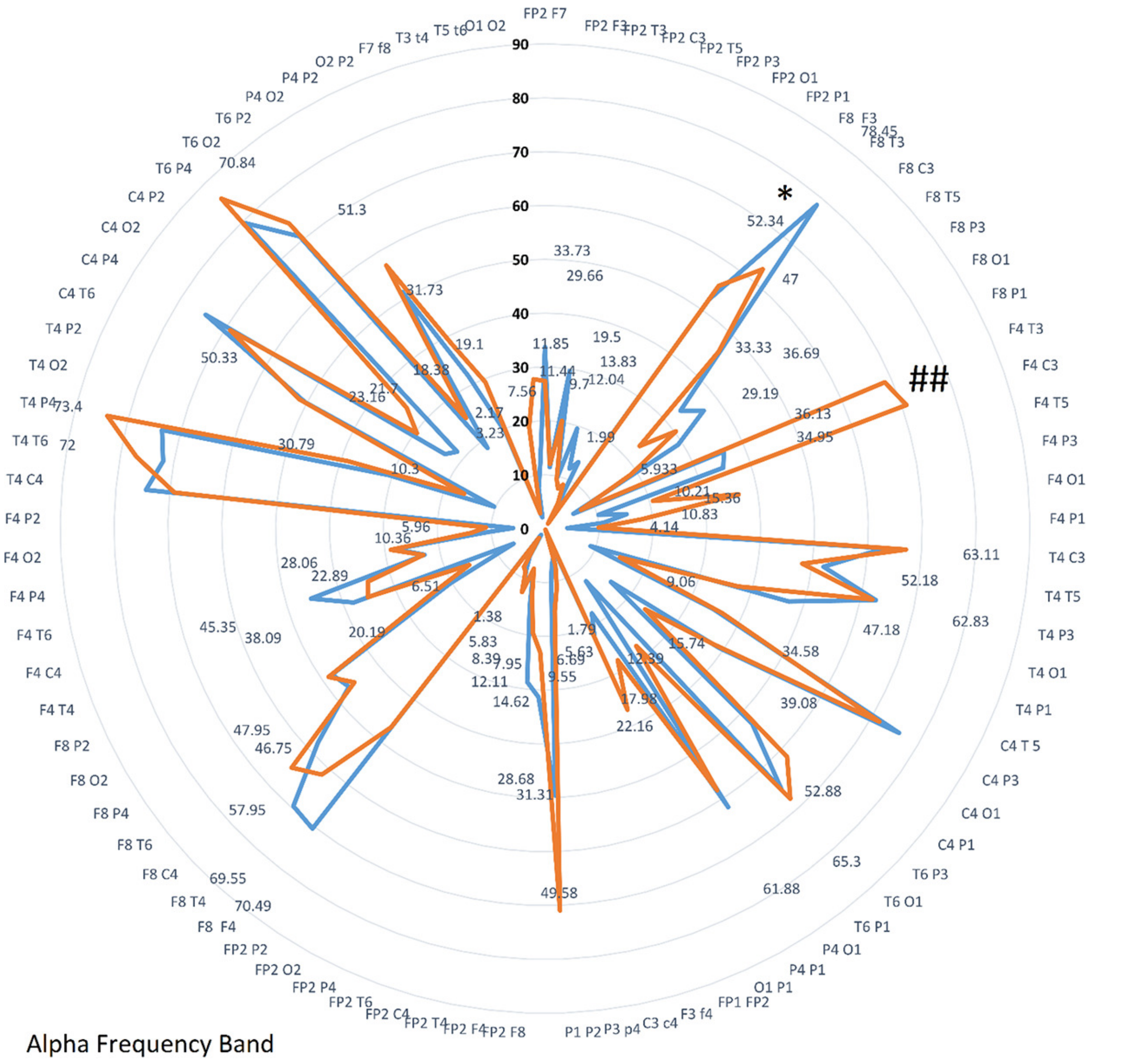

Fig. 3. Spiderweb chart plot of absolute power values for the alpha frequency band upon decision making (orange) and during resting state (blue) QEEG data. Analysis revealed higher alpha power during decision making task at F4–C3 dipoles compared with the resting state, ##$p < 0.01$. The F8–T3 dipole, however, showed the alpha power to dominate the resting state when compared to task-positive epochs, *$p < 0.05$. Values are presented as μV^2. FP: frontopolar, C: central, F: frontal, P: parietal, T: temporal and O: occipital.

analyses, beta power was found to be predominantly higher in the resting state than during DM epochs in F8–T3 [$t(5) = 2.72$, 95%CI = (0.034)–(2.37), $p = 0.008$], F8–F4 [$t(5) = 2.93$, 95%CI = (−2.66)–(−0.47), $p = 0.006$], F4–C4 [$t(5) = 3.11$, 95%CI = (0.83)–(1.3), $p = 0.004$], C4–P4 [$t(5) = 2.22$, 95%CI = (−1.46)–(−0.07), $p = 0.03$] and FP2–F3 [$t(5) = 2.16$, 95%CI = (−1.54)–(0.04), $p = 0.04$].

A fast Fourier transform (FFT) relative power analysis revealed increased alpha band power in the right centroparietal region during DM versus resting states. Additionally, relative beta power was diminished in the FP2 region during DM epochs. Such a decrease was evident at FP1 across high beta band frequency.

In terms of the FFT power ratio, delta/theta and delta/alpha ratios were increased in FP1 during DM epochs. Moreover, centroparietal regions showed a rise in the alpha/beta and alpha/high beta power ratio.

Fig. 5 demonstrates the spatial distribution and connectivity brain maps for resting states (section (A)) versus the grand average for the six DM blocks (section (B)). They suggested lower than expected beta power in the anterior brain regions when compared with occipital and centroparietal areas. This indicates that perhaps the DM process in the subject was more of an automatic and less cognitive in nature and regulated by subcortical (corticostrial) networks rather than cortico-cortical pathways. Interestingly, beta coherence in anterior brain regions diminished during DM epochs (grand average for six blocks, section (B), lower panel) when compared with the resting state (Section (A), lower panel) (Fig. 5).

With regard to the autonomic response data upon DM blocks, Fig. 6 showed increased HRV and the inter-beat group changes but

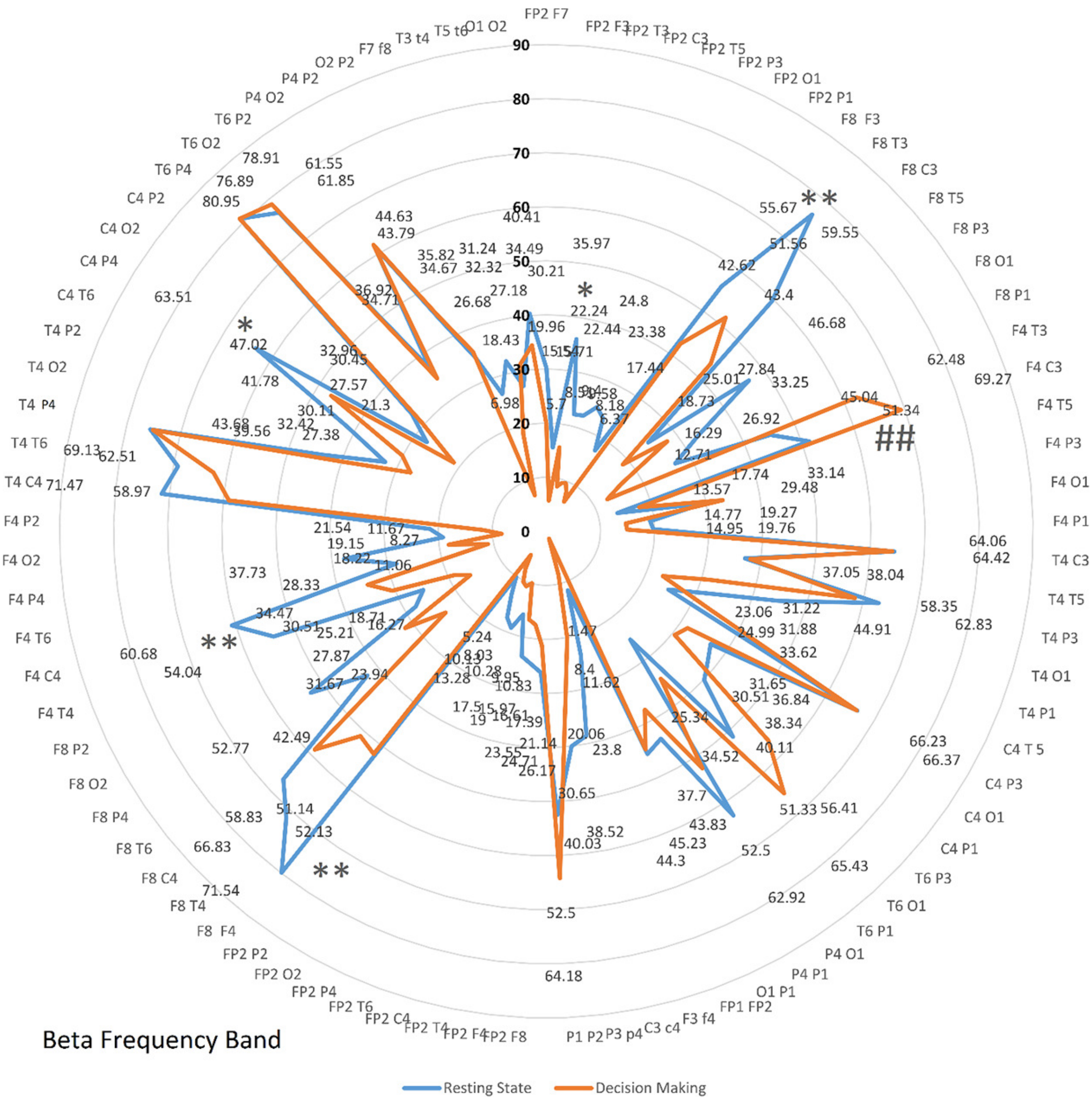

Fig. 4. Spiderweb chart plot of absolute power values for the beta frequency band upon decision making (orange) and during resting state (blue) QEEG data. Analysis revealed higher beta power during the resting state when compared with DM epochs at F8–T3, F8–F4, F4–C4, C4–P4, and FP2–F3. $*p < 0.05$, $**p < 0.01$, $\#\#p < 0.01$. Values are presented in μV^2. FP: frontopolar, C: central, F: frontal, P: parietal, T: temporal and O: occipital.

not GSR in DM blocks as highlighted (yellow). This suggests an autonomic component is involved when the subject is engaged (even subcortically) in a DM task (Fig. 6).

Fig. 7 illustrates an EEG source connectivity analysis. As outlined in the Methods section, an Infomax-based ICA decomposition algorithm using EEGLAB in MATLAB yielded 22 artifact-free components. Based on this analysis, the sources of information flow during a DM block were localized at components three, four, 13, 14, 15 and 16 which were anatomically linked to the left ventromedial prefrontal cortex (vmPFC) and right occipital and right medial temporal cortices. Alternatively, information flow sinks were localized at components 9, 11, 19 and 22, which were linked to the left orbitofrontal cortex (OFC), left PPC and right intraparietal sulcus (IPS). It was demonstrated to be the case that information flow during DM blocks was more from posterior towards anterior brain regions.

4. Discussion

The case study reported here was an attempt to investigate the plausible cortical networks potentially involved in DM tasks while a well-trained eight year old boy was engaged in chess play against a computer. Results from QEEG analysis indicated a lower power spectral density for higher frequency band power in the right hemisphere during DM epochs. Further analyses suggested that the information flow during DM blocks in this particular case were more from posterior towards anterior brain regions.

The inferior frontal gyrus has also been proposed to be centrally involved in DM processes [19]. In the present investigation however,

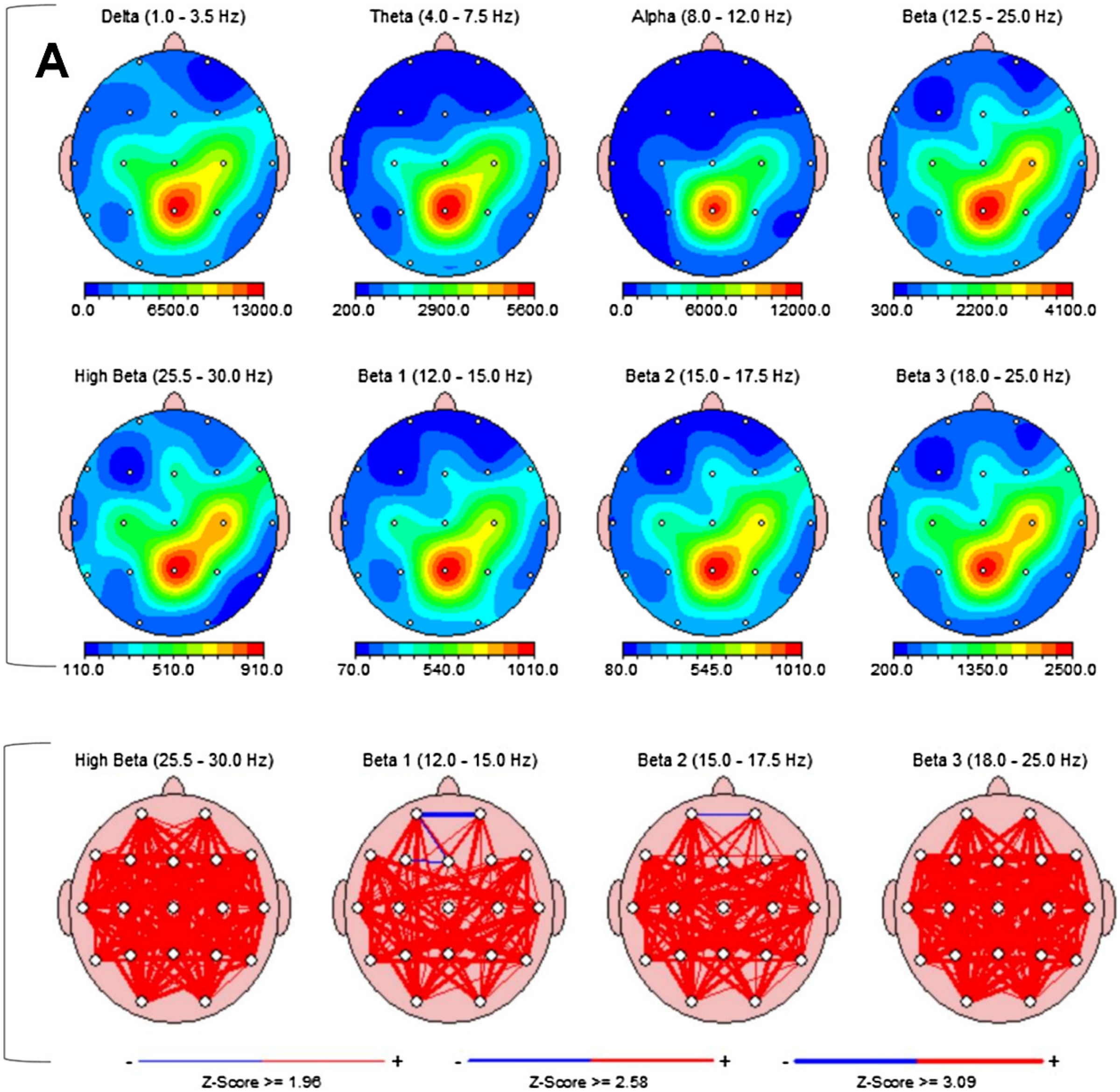

Fig. 5. QEEG topographical spectral brain maps. Analysis demonstrated absolute power values across spectra during resting state (section (A), upper panel) and decision making QEEG data (panel (B), upper panel). Resting state QEEG centroparietal activity is compatible with default mode network activity. Grand average for the six decision making blocks (section (B)) suggest lower than expected beta power in the anterior brain region rather than in the occipital and centroparietal areas. The lower panels in sections (A) and (B) give resting state and decision making beta coherence maps indicating a frontal beta hypocoherence during task-positive rather than resting states.

predominant theta frequency during DM epochs was observed in the right inferior frontal dipole. The hypothetical explanation for this observation may depend upon the role of dorsolateral prefrontal cortex and inferior frontal gyrus in the process of DM when cognitive control plays a central role [20]. This was found to be less the case when the subject was engaged in critical DM processes. The neural correlates of decision making are known to involve at least the anterior cingulate cortex, middle frontal gyrus, and inferior frontal gyrus/insula, with recent insights suggesting that decisions may emerge from distributed processes [19, 21].

Some earlier reports have indicated a role for left parietal theta power as a correlate of memory retrieval and DM [21, 22]. This study was in agreement with such results as a major sink, of information flow identified by QEEG analysis, was found in the left posterior parietal cortex (PPC). Indeed, unraveling the neural mechanism of this result may help explain key electrophysiological determinants of DM. As outlined in the Results section, electrophysiological differences associated with decision-making epochs mainly corresponded to the distribution and power of the theta frequency band in fronto-central and posterior parietal cortices. Based on these QEEG findings and source connectivity analysis, it is proposed that a neural model of a more automatic and less cognitive nature regulates the process of DM in the elite chess player tested.

Studies have considered chess as a suitable task paradigm for evaluation of the brain activity of a players under a combination of ambiguous circumstances and time pressure. For instance, a number

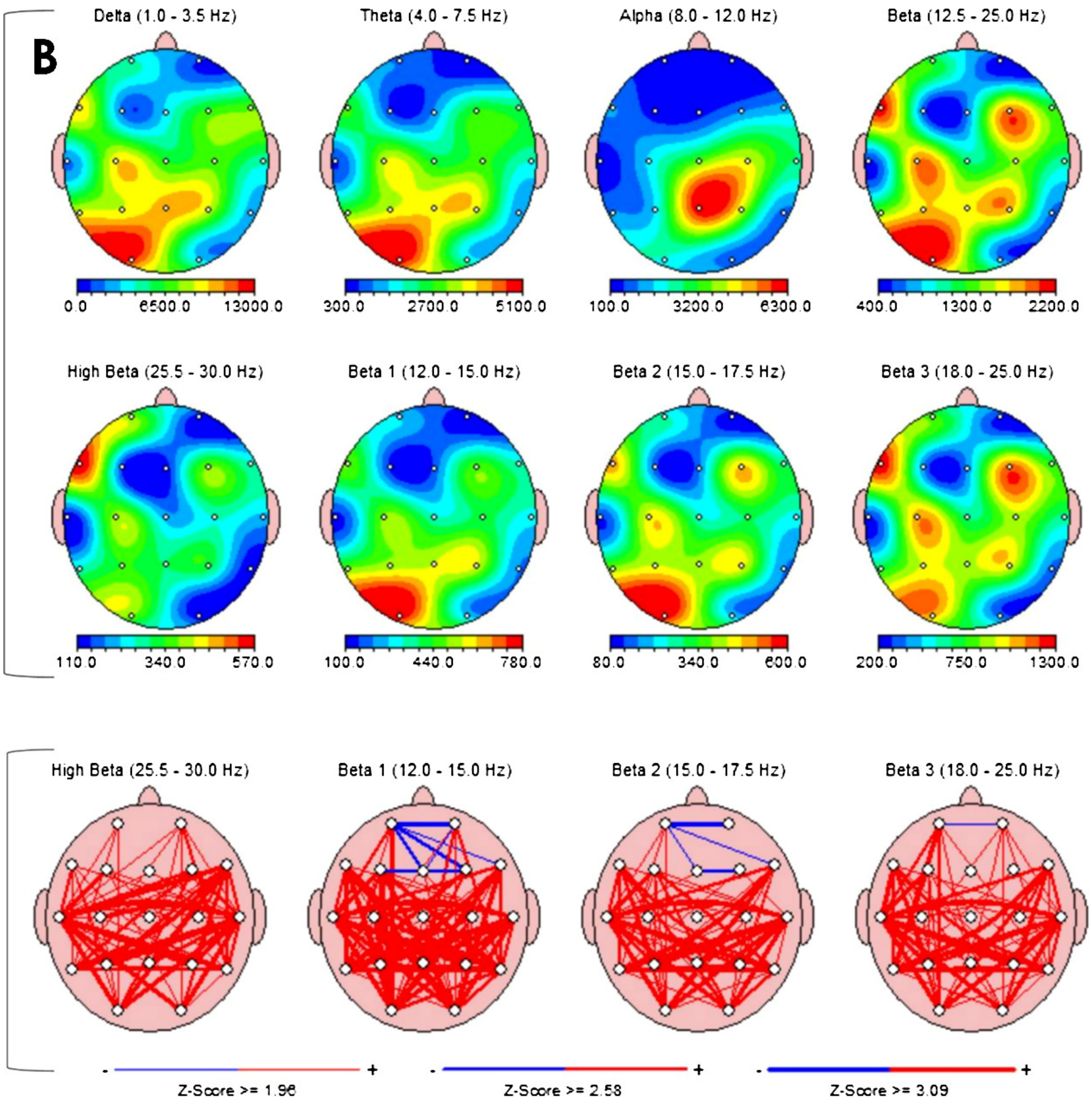

Fig. 5. (Continued.)

of neuroimaging investigations using functional magnetic resonance imaging (fMRI) aimed to localize the neural activity associated with perceptual DM. According to such evidence, cortical and subcortical brain regions and structures including the frontal and parietal cortices, thalamus, and striatum were found to be largely involved in modulating the accuracy and uncertainty of decisions [23–26]. In other well-designed studies, the memory recall of expert chess players was compared with that of beginners or less skilled players with whole-brain analysis conducted particularly on regions of interest such as the anterior cingulate cortex (ACC), bilateral intraparietal sulci (IPS), bilateral ventromedial and dorsolateral prefrontal cortices (vmPFC and dlPFC) and prefrontal cortices (PFC). Results from such studies of chess player brains corroborated that components of the frontoparietal network (FPN) are not only linked to consciousness and attention but also working memory [5, 7, 23]. Despite that, in this case study, the FPN was shown to be less involved once a well-trained chess player was making critical decisions. Instead, centroparietal areas were found to show a higher amplitude of the beta frequency band in QEEG and the sinks for information flow (estimated through ICA) turned out to be the left PPC and right IPS.

Recording tools such as EEG are not only less costly and more convenient to administer, but also capable of providing proper temporal resolution, hence they may be considered appropriate for addressing the temporal sequencing of DM signals [27]. For instance, a computational model-based approach to EEG data acquired during a simple binary choice task have been shown to yield dependable data on the temporal sequence of information flow in the brain [28, 29].

In studies which examined pattern recognition of four simple conditions in chess, evoked coherences of EEG signals were found to be sensitive to sensory as well as mental activity (theta and beta coherence, respectively). Meanwhile, beta coherence was to a marked extent dependent on the type of task [30].

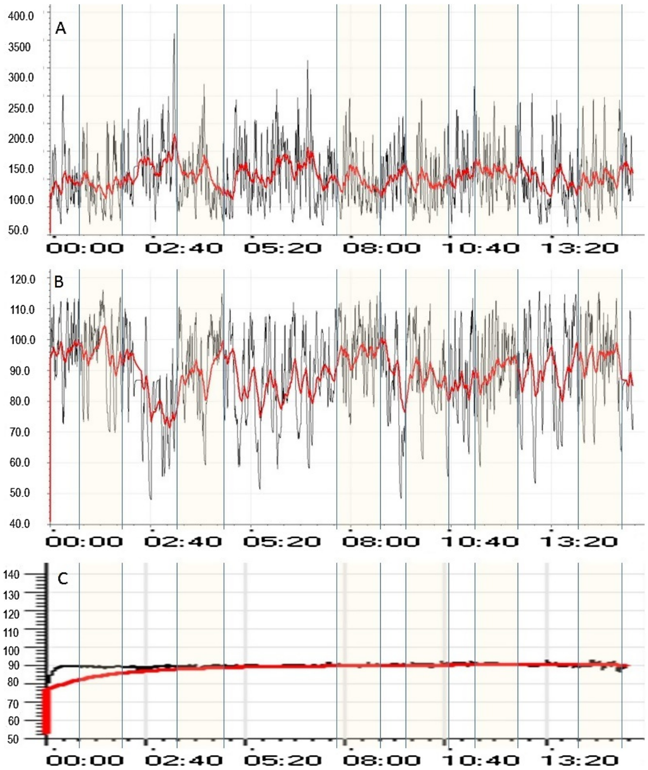

Fig. 6. Autonomic response during the decision making task. Panels (A)–(C) give heart rate variability (HRV), pNN50 (number of pairs of successive NN intervals that differ by more than 50 ms), and GSR (in μSiemens). Yellow color indicates the decision making (DM) blocks from which EEG data were extracted and analyzed. Despite no significant difference in GSR between DM and non-DM blocks, there was an apparent increase in HRV and PNN50 in the DM blocks. This suggests involvement of an autonomic component when the subject was engaged in the DM task.

In the case of perceptual DM, analysis is more error-prone, especially near the threshold. Despite the internal noise proposed to exist in neural systems, which seems to be responsible for such errors, it appears that a mixture of bottom-up and top-down sources drive this potential complexity [31]. Such complexity when interpreting data should be considered if EEG is to be used as the method of choice for neurocognitive studies.

5. Conclusion

The present QEEG findings suggest a lower cognitive load during a DM task for the particular subject, based on the dominance of right and posterior alpha/theta versus beta frequency bands. Consequently, FPN was shown to be less involved once the subject was involved in a critical DM. These data may suggest that perhaps an immature system responds preferentially to outcomes only so as to initiate a fast automatic alertness response after becoming an expert chess player.

Though this research opens up new avenues for the investigation of the neural system underlying normal DM, future studies should demonstrate the level of involvement of FPN and subcortical nuclei when elite versus novice chess players engage in critical DM tasks. The combined use of advanced neurotechnological tools such as fMRI, functional near infra-red spectroscopy (fNIRS) and magnetoencephalography (MEG) offer novel opportunities for greater in-depth investigation of such issues.

Acknowledgments

Authors would like to thank Ms. S. Safaie for her assistance with this report.

Conflict of Interest

All authors declare no conflicts of interest.

References

[1] Jollans L, Whelan R, Venables L, Turnbull OH, Cella M, Dymond S (2016) Computational EEG modelling of decision making under ambiguity reveals spatio-temporal dynamics of outcome evaluation. *Behavioural Brain Research* **321**, 28-35.

[2] Forbes DP, Milliken FJ (1999) Cognition and Corporate Governance: Understanding Boards of Directors as Strategic Decision-Making Groups. *Academy of Management Review* **24(3)**, 489-505.

[3] Mahmoud M, Liu Y, Hartmann H, Stewart S, Wagener T, Semmens D, Stewart R, Gupta H, Dominguez D, Dominguez F (2009) A formal framework for scenario development in support of environmental decision-making. *Environmental Modelling & Software* **24(7)**, 798-808.

[4] Connors MH, Burns BD, Campitelli G (2011) Expertise in complex decision making: the role of search in chess 70 years after de Groot. *Cognitive Science* **35(8)**, 1567-1579.

[5] Eisele P (2004) Judgment and decision-making: experts' and novices' evaluation of chess positions. *Perceptual & Motor Skills* **98(1)**, 237-248.

[6] Gustafson DH, Bosworth K, Hawkins RP, Boberg EW, Bricker E (1992) CHESS: a computer-based system for providing information, referrals, decision support and social support to people facing medical and other health-related crises. In, Proceedings of the Annual Symposium on Computer Application in Medical Care (p. 161-165). American Medical Informatics Association.

[7] Sigman M, Etchemendy P, Slezak DF, Cecchi GA (2010) Response time distributions in rapid chess: a large-scale decision making experiment. *Frontiers in Neuroscience* **4**, 60.

[8] Stanovich KE, West RF (2000) Individual differences in reasoning: implications for the rationality debate? *Behavioral & Brain Sciences* **23(5)**, 665-726.

[9] Kørnøv L, Thissen WA (2000) Rationality in decision-and policy-making: implications for strategic environmental assessment. *Impact Assessment and Project Appraisal* **18(3)**, 191-200.

[10] Sternberg, Robert J (2000) The ability is not general, and neither are the conclusions. *Behavioral & Brain Sciences* **23(5)**, 697-698.

[11] Burns BD (2004) The effects of speed on skilled chess performance. *Psychological Science* **15(7)**, 442-447.

[12] Hl VDM, Wagenmakers EJ (2005) A psychometric analysis of chess expertise. *American Journal of Psychology* **118(1)**, 29-60.

[13] Ashjazadeh N, Boostani R, Ekhtiari H, Emamghoreishi M, Farrokhi M, Ghanizadeh A, Hatam G, Hadianfard H, Lotfi M, Mortazavi SMJ (2014) Operationalizing Cognitive Science and Technologies' Research and Development; the "Brain and Cognition Study Group (BCSG)" Initiative from Shiraz, Iran. *Basic & Clinical Neuroscience* **5(2)**, 104.

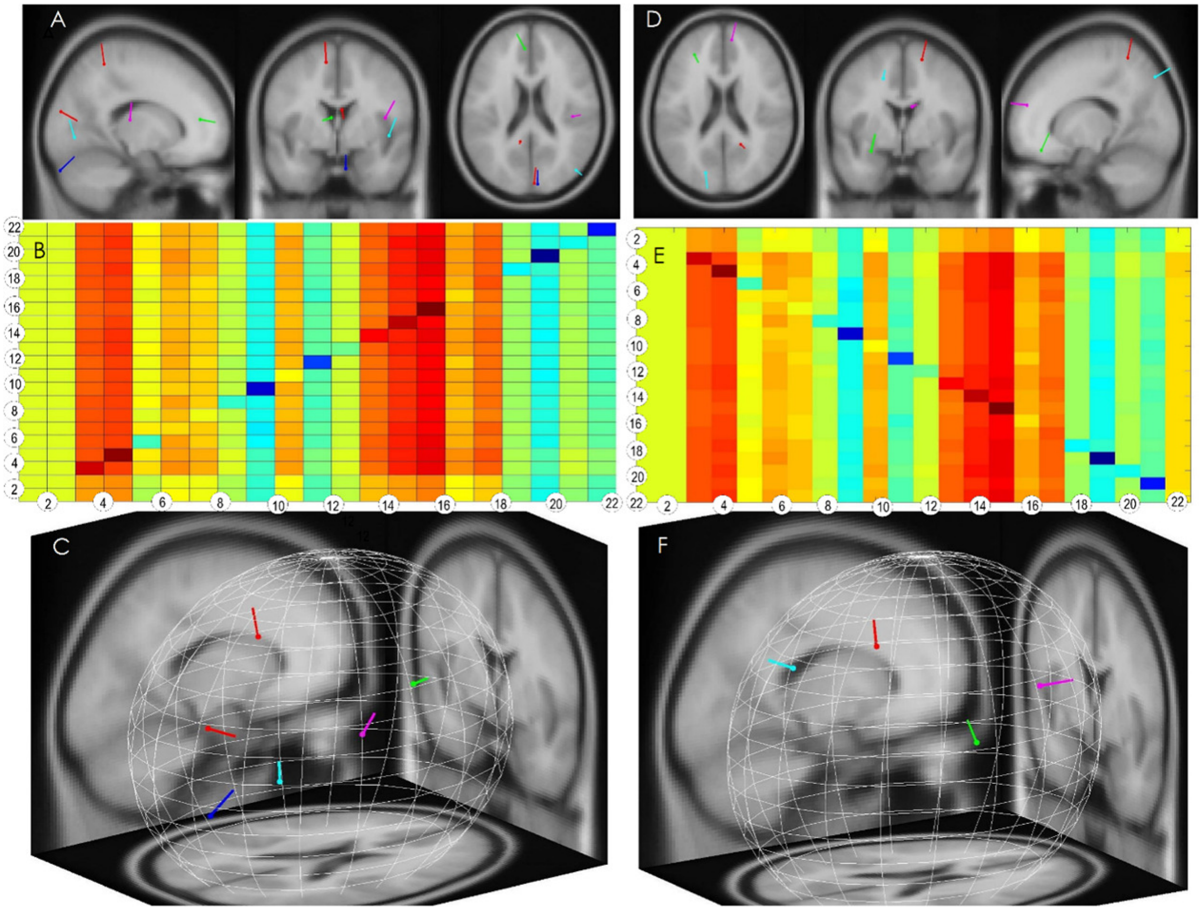

Fig. 7. Information flow between major sources and sinks during critical decision making. (A) (left to right): Position of information sources in sagittal, coronal, and transverse sections. (B): Color matrix for information flow between all signal sources. Each square represents the information flow difference between resting and DM states for a specific pair of signal sources. For example, the red elements (four, three) indicate increased information flow and causal effect of signal source three on signal source four during DM epochs. (C): Position of information sources in 3D space. (D) (left to right): Position of "information sinks" in sagittal, coronal, and transverse sections. (E): Reciprocal color matrix (versus (B)) for information flow between all signal sources. (F): Position of information sinks in 3D space. Sources and sinks were identified by thresholding the magnitude of their causal effect. Sources of information flow during DM blocks were localized at components 3, 4, 13, 14, 15 and 16 (anatomically linked to the left vmPFC, right occipital and right medial temporal cortices); the information flow sinks were localized at components 9, 11, 19 and 22 (anatomically linked to the left OFC, left PPC and right IPS).

[14] Nazaraghaie F, Torkamani F, Kiani B, Torabi-Nami M (2015) EEG-guided meditative training through geometrical approach: an interim analysis. *Avicenna Journal of Phytomedicine* **5**, 146.

[15] Benabdelkader C, Yacoob Y (2010) Statistical estimation of human anthropometry from a single uncalibrated image. *Computational Forensics*, 200-220.

[16] Arnaud D, Tim M, Christian K, Zeynep AA, Nima BS, Andrey V, Scott M (2011) EEGLAB, SIFT, NFT, BCILAB, and ERICA: New Tools for Advanced EEG Processing. *Computational Intelligence & Neuroscience* **2011**, 130714.

[17] Mullen TR (2014) The dynamic brain: Modeling neural dynamics and interactions from human electrophysiological recordings. *University of California, San Diego, ProQuest Dissertations Publishing*.

[18] Korzeniewska A, Mańczak M, Kamiński M, Blinowska KJ, Kasicki S (2003) Determination of information flow direction among brain structures by a modified directed transfer function (dDTF) method. *Journal of Neuroscience Methods* **125(1,2)**, 195-207.

[19] Thielscher A, Pessoa L (2007) Neural correlates of perceptual choice and decision making during fear-disgust discrimination. *Journal of Neuroscience* **27(11)**, 2908-2917.

[20] Cieslik CE, Zilles K, Caspers S, Roski C, Kellermann TS, Jakobs O, Langner R, Laird AR, Fox PT, Eickhoff SB (2013) Is There "One" DLPFC in Cognitive Action Control? Evidence for Heterogeneity From Co-Activation-Based Parcellation. *Cerebral Cortex* **23(11)**, 2677-2689.

[21] Zhang D, Gu R, Broster LS, Jiang Y, Luo W, Zhang J, Luo Y (2014) Linking brain electrical signals elicited by current outcomes with future risk decision-making. *Frontiers in Behavioral Neuroscience* **8**, 84.

[22] Jacobs J, Hwang G, Curran T, Kahana MJ (2006) EEG oscillations and recognition memory: Theta correlates of memory retrieval and decision making. *Neuroimage* **32(2)**, 978-987.

[23] Grinband J, Hirsch J, Ferrera, P. V (2006) A Neural Representation of Categorization Uncertainty in the Human Brain. *Neuron* **49(5)**, 757-763.

[24] Heekeren HR, Marrett S, Bandettini PA, Ungerleider LG (2004) A general mechanism for perceptual decision-making in the human brain. *Nature* **431(7010)**, 859-862.

[25] Paulus MP, Hozack N, Frank L, Brown GG (2002) Error Rate and Outcome Predictability Affect Neural Activation in Prefrontal Cortex and Anterior Cingulate during Decision-Making. *Neuroimage* **15(4)**, 836-846.

[26] Shadlen MN, Newsome WT (2001) Neural basis of a perceptual decision in the parietal cortex (Area LIP) of the rhesus monkey. *Journal of Neurophysiology* **86(4)**, 1916.

[27] Alipour A, Mojdehfarahbakhsh A, Tavakolian A, Morshedzadeh T, Asadi M, Mehdizadeh A, Nami M (2016) Neural communication through theta-gamma cross-frequency coupling in a bistable motion perception task. *Journal of Integrative Neuroscience* **15(4)**, 539-551.

[28] Kyathanahally S, Franco-Watkins A, Zhang X, Calhoun V, Deshpande G (2016) A realistic framework for investigating decision-making in the brain with high spatio-temporal resolution using simultaneous EEG/fMRI and joint ICA. *Journal of Biomedical & Health Informatics* **21(3)**, 814-825.

[29] Larsen T, O'Doherty JP (2014) Uncovering the spatio-temporal dynamics of value-based decision-making in the human brain: a combined fMRI–EEG study. *Philosophical Transactions of the Royal Society of London* **369(1655)**, 315-318.

[30] Volke HJ, Dettmar P, Richter P (2002) On-coupling and off-coupling of neocortical areas in chess experts and novices as revealed by evoked EEG coherence measures and factor-based topological analysis–a pilot study. *Journal of Psychophysiology* **16(1)**, 23-36.

[31] Amitay S, Guiraud J, Sohoglu E, Zobay O, Edmonds BA, Zhang YX, Moore DR (2013) Human decision making based on variations in internal noise: an EEG study. *Plos One* **8(7)**, e68928.